Ion-Exchange Equilibria of Pb^{2+}, Ni^{2+}, and Cr^{3+} Ions for H^+ on Amberlite IR-120 Resin

Manuel Carmona,[†] Jolanta Warchoł,[‡] Antonio de Lucas,[†] and Juan F. Rodriguez*,[†]

Department of Chemical Engineering, University of Castilla—La Mancha, Avda. de Camilo José Cela s/n, 13004 Ciudad Real, Spain, and Department of Water Purification and Protection, Rzeszŏw University of Technology, 6 Powstańcŏw Warszawy Str., 35-959 Rzeszów, Poland

A study of the binary cation-exchange equilibria between H^+-form Amberlite IR-120 resin and aqueous solutions of lead, nickel, and chromium nitrates at pH < 3 has been made. Experiments were carried out at (283, 303, and 323) K with solutions having total cation concentrations of 0.1 eq·L^{-1}. The experimental equilibrium data have been satisfactorily correlated using the homogeneous mass action law model (LAM). This model assumes nonideal behavior for both the solution and the solid phase. Wilson and Pitzer equations have been used to calculate activity coefficients in the solid and liquid phases, respectively. The standard enthalpy ΔH°_{AB} and the standard entropy ΔS°_{AB} were determined. The values of both the thermodynamic constant and standard Gibbs free energy ΔG°_{AB} demonstrate temperature dependence. The rise in temperature caused a slight increase in the value of the equilibrium constant (K_{AB}) for the ion exchange of all heavy metal ions tested in this study. According to equilibrium constants obtained, the Amberlite IR-120 exhibits the following order of selectivity, $Cr^{3+} > Pb^{2+} > Ni^{2+}$, in all the ranges of the temperatures studied in agreement with the rule of higher selectivity at higher counterion charge.

Introduction

Heavy metals such as chromium(III), nickel(II), and lead(II) are considered high priority environmental pollutants. Their concentration in industrial effluents (e.g., electroplating, battery and chemical manufacture, mining, metal finishing, forging, and petroleum refining) is undesirable due to their accumulation in soil and plants as well as contamination of aquatic systems. To avoid the presence of these kinds of compounds in the aquatic systems is nowadays an environmental challenge since, even in trace amounts, these toxic and carcinogenic ions can be harmful to aquatic life and the human body.[1–3] There are many methods that can be applied to the removal of heavy metals: chemical precipitation (using lime and caustic soda), alum and iron coagulation, ion exchange, adsorption, evaporation, filtration, membrane separation, electrochemical processes, reverse osmosis, and biomass.[4–6] However, in some cases, especially at low metal concentrations, the practical application of enumerate methods can be ineffective, economically unfavorable, or technically complicated. Ion exchange has been developed as an economically feasible alternative for treating wastewater over the past few decades. This technology allows for reaching the maximum permissible concentrations for heavy metals in effluents with the increase in environmental awareness and governmental policies. Moreover, because of the mild operating conditions, it can be utilized as supporting systems for conventional purification technology. Pollutant ions present in the stream are replaced by noncontaminant ions released from the ion exchanger.[7,8] Once the capacity of the ion exchanger has been spent by entering ions uptake, it can be regenerated with a highly concentrated regenerant agent, to restore the initial ionic form and continue again with the removal process.[9,10]

Several natural ion exchangers such as zeolitic and clay minerals, byproduct, and wastes from agricultural or forest industries[11] can be used for heavy metal removal. However, the complexity of natural materials has made them unpredictable regarding the impact of existing conditions on the binding mechanism, capacity, and affinity. In opposite synthetic resins such as Amberlite IRA-120 and IRN97H, Amberjet 1200H and 1500H (strong cationic resin),[4,12,13] chelating exchange resins (Lewatit TP-207, Diaion CR11),[4,14,15] weak cationic resins (Amberlite IRC86),[15] and synthetic zeolite (NaP1)[4] exhibit high heavy metal capacity, resistance against chemical and physical stress, as well as mechanical stability.[16]

The design and efficient operation of ion-exchange processes require equilibrium data for use in kinetic and mass transport models. Thus, the modeling of the ion-exchange equilibrium is an a priori step for successful optimization of the design and operation conditions of a fixed bed ion-exchange column or for its scaling up. The equilibrium model can then be used to predict the performance of the ion-exchange process under a range of operating conditions. Unfortunately, the collected data presented in the literature are not complete or based on models that are not always adequate for process mechanism which means that the design of ion-exchange plants is still rather empirical.

In previous studies, it was indicated that strong acid resins such as Amberlite IR-120 may be used for the recovery of toxic metals (Cu^{2+}, Cd^{2+}, Zn^{2+}) at certain conditions, and the entire study of the equilibrium and kinetic behavior was carried out for the resin in both H^+ and Na^+ forms. The experimental data were fitted to theoretical physicochemical models, and the parameters were obtained.[17,18] Finally, these parameters were used to predict the breakthrough points for the load process and the minimum regenerant agent required for reusing the column.[12]

* To whom correspondence should be addressed. Phone: 34-902204100. Fax: 34-926-295318 Email: juan.rromero@uclm.es.
[†] University of Castilla—La Mancha.
[‡] Rzeszŏw University of Technology.

10.1021/je8000552 CCC: $40.75
Published on Web 05/10/2008

Table 1. Parameters of the Pitzer Limiting Law[30,31]

species	βca^0	βca^1	Cca^{φ}
HNO_3	0.1119	0.3206	−0.001
$Pb(NO_3)_2$	−0.03615	0.2850	0.0053
$Ni(NO_3)_2$	0.3535	1.6049	−0.101
$Cr(NO_3)_2$	0.7040	5.1847	−0.059

The goal of this work is to obtain the ion-exchange equilibrium data for the systems H^+/Pb^{2+}, H^+/Ni^{2+}, and H^+/Cr^{3+} on the strong acid resin Amberlite IR-120 in aqueous media at temperatures of (283, 303, and 323) K and a total concentration in the solution of 0.1 eq·L^{-1}. Similar to a previous publication,[17] the model based on the homogeneous mass action law was employed to obtain the thermodynamic equilibrium constant and the binary interaction parameters. Wilson and Pitzer equations were used to consider the nonideal behavior of the ions in the solid and liquid phases, respectively, in the same way as in previous works in the field.[19–22]

Experimental Section

Chemical. All solutions used in the study were prepared from analytical grade chemicals: $Pb(NO_3)_2$, $Ni(NO_3)_2 \cdot 6H_2O$, $Cr(NO_3)_3 \cdot 9H_2O$ (quality PA, supplied by Panreac), and high-quality deionized water with a conductivity value lower than 1 $\mu S \cdot cm^{-3}$.

The cationic resin Amberlite IR-120 supplied by Rhom & Haas was used as the ion exchanger. The physical properties of the resin have been presented elsewhere.[23] Prior to the laboratory tests, the resin was pretreated and regenerated to convert it to the H^+-form as described by de Lucas et al. [24] The water content in the resin was found by thermogravimetry (Perkin-Elmer Thermal Analysis Controller TAC 7/DX) to be 35.34 % w/w.

Procedure. The experimental set consisted of nine 0.25 L glass containers, hermetically sealed and submerged in a temperature-controlled thermostatic bath. The fixed temperature [(283, 303, and 323) K] was kept constant with maximum deviations of ± 0.1 K. Different known masses of resin, in the H^+-form, were put in contact with aqueous solutions of metal ions in the presence or absence of known concentrations of HNO_3 to ensure the same initial solution phase charge concentration of total normality equal to 0.1 eq·L^{-1}. The precision of resin weighing was ± 0.0001 g. The solution pH value was always lower than 3 to avoid hydroxyl complex formation and thus possible metal precipitation.

Equilibrium resin loading data were generated for the H^+/Pb^{2+}, H^+/Ni^{2+}, and H^+/Cr^{3+} systems. The suspension formed by the resin and solution were vigorously agitated by means of a multipoint magnetic stirrer for 24 h. Preliminary tests confirmed that this period was enough to ensure that equilibrium had been attained. At the end of this period, the mixtures were filtered to remove the solid phase from the liquid by filtration.

The liquid phase was analyzed for metal content by an inductively coupled plasma spectrophotometer sequential ICP-AES (Varian), and both initial and equilibrium pH were measured with a Basic 20 (CRISON) pH meter.

The resin phase composition was determined by mass balance from initial and equilibrium compositions of the liquid phase, according to eq 1

$$q^* = \frac{V}{W}(C_0 - C^*) \tag{1}$$

where C_0 and C^* are the initial and equilibrium concentration of metal in the liquid phase (meq·L^{-1}), respectively; and q^* denotes the resin-phase equilibrium concentration of metal (meq·g^{-1} dry resin). V and W are the volume of solution (L) and the weight of dry ion-exchange resin (g).

Model and Prediction. An ion-exchange reaction is defined as a reversible exchange of ions between a liquid phase containing counterions, which are different from those initially in the solid phase. Let us consider the following ion-exchange process for a binary system (eq 2) where the ion exchanger (r) is initially in the A-form and the counterion in the solution is B. Counterion exchange occurs, and the ion A in the ion exchanger is partially replaced by B

$$\beta A_r^{\alpha+} + \alpha B_s^{\beta+} \leftrightarrow \beta A_s^{\alpha+} + \alpha B_r^{\beta+} \tag{2}$$

where α and β are the valences of the ionic species A and B, respectively.

In the equilibrium state, the solid and liquid phases contain both competing counterion species, A and B. Electroneutrality is necessarily maintained in this reaction whether in the ion exchanger or in the aqueous solution. This indicates that counterion exchange occurs in equivalents, and the ionic concentration for a binary system can be expressed as an ionic fraction as follows

$$x_A = \frac{C_A^*}{N};\ x_B = \frac{C_B^*}{N} \tag{3}$$

$$y_A = \frac{q_A^*}{q_0};\ y_B = \frac{q_B^*}{q_0} \tag{4}$$

where y_B and x_B represent the fraction of the ion B in the solid and liquid phase, respectively. N is the total normality of the ions in the solution phase (eq·L^{-1}), and q_0 is the useful capacity of the resin in the system studied (eq·g^{-1} of dry resin).

The important factor that should be considered in a comprehensive theory of ion exchange is nonideal behavior of ions in the solid and liquid phases. It can result from an ion−ion and ion−solid interaction, ionic charge, ionic radius, and other molecular constants.[25] Therefore, the equilibrium constant for the exchange reaction (2) assuming real behavior for both phases could be expressed by the following equation

$$K_{AB}(T) = \frac{y_B^{\alpha}}{(1-y_B)^{\beta}} \cdot \frac{(1-x_B)^{\beta}}{x_B^{\alpha}} \cdot \left(\frac{\gamma_A}{\bar{\gamma}_A}\right)^{\beta} \cdot \left(\frac{\bar{\gamma}_B}{\gamma_B}\right)^{\alpha} \cdot \left(\frac{q_0}{N}\right)^{\alpha-\beta} \tag{5}$$

where $\bar{\gamma}$ and γ are the activity coefficients of each ion in the ion exchanger and in the solution, respectively.

Liquid phase activity coefficients in the mixed solution containing cations c and anions a were calculated from the Pitzer limiting law.[26,27] If the mixing terms are considered to be small, the equation for the cation M can be expressed as[27–30]

$$\ln \bar{\gamma}_{\mathrm{M}} = z_{\mathrm{M}}^2 F + \sum_a m_a(2B_{\mathrm{M}a} + ZC_{\mathrm{M}a}) + |z_{\mathrm{M}}| \sum_c \sum_a m_a m_c C_{ca} \tag{6}$$

where c and c' are cations and a and a' are anions and m_i is the molality of the ion i. The charge is indicated by z_{M}. The quantity F includes the Debye−Hückel term and other terms as follows

$$F = -A_{\varphi}[I^{1/2}/(1 + bI^{1/2}) + (2/b)\ln(1 + bI^{1/2})] + \sum_c \sum_a m_c m_a B'_{ca} \tag{7}$$

$$Z = \sum_i m_i |z_i| \tag{8}$$

$$I = 0.5 \sum_i m_i \cdot z_i^2 \tag{9}$$

where I is the ionic strength in the bulk phase in molal units. The sums over i include all solute species; uncharged species

Table 2. Comparison among Experimental and Predicted Ion-Exchange Equilibrium Data for Pb^{2+} on Amberlite IR-120

T/K = 283			T/K = 303			T/K = 323		
exptl		theor.	exptl		theor.	exptl		theor.
$x_{Pb^{2+}}$	$y_{Pb^{2+}}$	$y_{Pb^{2+}}$	$x_{Pb^{2+}}$	$y_{Pb^{2+}}$	$y_{Pb^{2+}}$	$x_{Pb^{2+}}$	$y_{Pb^{2+}}$	$y_{Pb^{2+}}$
0.0072	0.4314	0.4741	0.0051	0.4189	0.4593	0.0049	0.4367	0.4806
0.0314	0.6598	0.6424	0.0247	0.6752	0.6408	0.0269	0.6989	0.6786
0.0735	0.7851	0.7244	0.0677	0.8204	0.7382	0.0732	0.7911	0.7809
0.2111	0.8540	0.8360	0.1971	0.8511	0.8515	0.2113	0.8593	0.8737
0.2791	0.8668	0.8646	0.2676	0.8159	0.8859	0.3382	0.9122	0.9083
0.3435	0.8876	0.8839	0.3199	0.8774	0.8946	0.4402	0.9281	0.9294
0.4472	0.9130	0.9094	0.4168	0.8980	0.9172	0.6768	0.9348	0.9658
0.6632	0.9444	0.9509	0.6186	0.9504	0.9509	0.8917	0.9424	0.9897
0.8772	0.9900	0.9828	0.8429	0.9570	0.9820	---	---	---

Table 3. Comparison among Experimental and Predicted Ion-Exchange Equilibrium Data for Ni^{2+} on Amberlite IR-120

T/K = 283			T/K = 303			T/K = 323		
exptl		theor.	exptl		theor.	exptl		theor.
$x_{Ni^{2+}}$	$y_{Ni^{2+}}$	$y_{Ni^{2+}}$	$x_{Ni^{2+}}$	$y_{Ni^{2+}}$	$y_{Ni^{2+}}$	$x_{Ni^{2+}}$	y_{Ni}^{2+}	$y_{Ni^{2+}}$
0.0174	0.4305	0.4460	0.0170	0.4333	0.4143	0.0166	0.4371	0.4444
0.0452	0.6356	0.6244	0.0468	0.6303	0.6126	0.0443	0.6296	0.6327
0.0883	0.7281	0.7292	0.0877	0.7427	0.7191	0.0846	0.7901	0.7413
0.2503	0.8178	0.8589	0.2352	0.9179	0.8542	0.2437	0.8615	0.8668
0.3268	0.8529	0.8879	0.3174	0.9026	0.8846	0.3351	0.8078	0.8955
0.3950	0.9075	0.9086	0.3947	0.9064	0.9068	0.3926	0.9174	0.9149
0.5446	0.9337	0.9404	0.5430	0.9387	0.9394	0.5406	0.9442	0.9445
0.7498	0.9882	0.9718	0.7774	0.9399	0.9746	0.7742	0.9417	0.9765
0.9865	0.9900	0.9986	0.9900	0.9465	0.9990	0.9855	1.0000	0.9987

Table 4. Comparison among Experimental and Predicted Ion-Exchange Equilibrium Data for Cr^{3+} on Amberlite IR-120

T/K = 283			T/K = 303			T/K = 323		
exptl		theor.	exptl		theor.	exptl		theor.
$x_{Cr^{3+}}$	$y_{Cr^{3+}}$	$y_{Cr^{3+}}$	$x_{Cr^{3+}}$	$y_{Cr^{3+}}$	$y_{Cr^{3+}}$	$x_{Cr^{3+}}$	$y_{Cr^{3+}}$	$y_{Cr^{3+}}$
0.0006	0.4327	0.4332	0.0005	0.4347	0.4352	0.0002	0.4376	0.4382
0.0144	0.7468	0.7474	0.0132	0.7686	0.7723	0.0115	0.7578	0.8034
0.0644	0.8153	0.8404	0.0635	0.8449	0.8605	0.0618	0.8625	0.8798
0.1876	0.8467	0.8957	0.1848	0.8694	0.9097	0.1757	0.9355	0.9204
0.2467	0.8488	0.9099	0.2480	0.8642	0.9232	0.2362	0.9234	0.9320
0.3088	0.8671	0.9218	0.3077	0.8697	0.9330	0.2970	0.9182	0.9413
0.4099	0.8727	0.9375	0.3909	0.8995	0.9445	0.3877	0.9062	0.9514
0.6059	0.8894	0.9581	0.6014	0.9086	0.9607	0.5716	0.9680	0.9637
0.8142	0.9900	0.9700	0.7998	0.9511	0.9766	0.7949	0.9730	0.9750

Table 5. Equilibrium Parameters of the Binary Systems H^+/Pb^{2+}, H^+/Ni^{2+}, and H^+/Cr^{3+} on the Resin Amberlite IR-120

system	T	K_{AB}			av. dev		
$(A^{\alpha+}/B^{\beta+})$	K	$(kg \cdot eq^{-1})^{\beta-\alpha}$	Λ_{AB}	Λ_{BA}	(%)	CAB^A	CAB^B
H^+/Pb^{2+}	283	3.5922	1.1328	1.8511	2.7612	276.2737	211.9431
	303	4.6650	1.1050	1.8115	4.4588	276.2735	211.9439
	323	5.8654	1.0808	1.7772	3.1011	276.2739	211.9427
H^+/Ni^{2+}	283	0.7450	0.6790	1.4935	2.0003	30.1237	22.6910
	303	0.9675	0.7292	1.2165	3.1868	30.1237	22.6967
	323	1.2164	0.7323	1.2183	3.1661	30.1238	22.6886
H^+/Cr^{3+}	283	4.2729	1.0740	1.0486	4.3276	33.9921	31.3932
	303	8.1539	1.0634	0.8463	3.7439	27.9802	31.3944
	323	14.3639	1.0757	1.0332	2.0365	34.3322	35.0398

do not contribute to I or Z. The double summation indices, $c < c'$ and $a < a'$, denote the sum over all distinguishable pairs of different cations or anions. The constant b is a universal parameter with the value 1.2 $kg^{1/2} \cdot mol^{-1/2}$, and the constant A_ϕ is dependent on the temperature with the following values 0.3821, 0.3949, and 0.4103 at (283, 303, and 323) K, respectively. B_{ca}' is the ionic strength derivatives of B_{ca}, and they are given by the following equations in terms of the commonly tabulated parameter $\beta^{(0)}{}_{ca}$ and $\beta^{(1)}{}_{ca}$.[27]

$$B_{ca} = \beta_{ca}^{(0)} + \beta_{ca}^{(1)} g(X) \tag{10}$$

$$B_{ca}^{'} = \beta_{ca}^{(1)} g^{'}(X)/I \tag{11}$$

where

$$X = \alpha \cdot I^{1/2} \tag{12}$$

$$g(X) = 2[1 - (1 + X)\exp(-X)]/X^2 \tag{13}$$

$$g^{'}(X) = -2[1 - (1 + X + X^2/2)\exp(-X)]/X^2 \tag{14}$$

The parameter C_{ca} is related to the commonly tabulated parameter $C^{\Phi}{}_{ca}$ by the equation:

$$C_{ca} = C_{ca}^{\varphi}/(2|z_c z_a|^{1/2}) \tag{15}$$

A value of 2.0 $kg^{1/2} \cdot mol^{-1/2}$ for α is recommended by Pitzer for several types of salts at 25 °C. This value can be used for all the electrolytes studied in this paper. Values for $\beta_{ca}^{(0)}$, $\beta_{ca}^{(1)}$, and Cca^{φ} are species-dependent, and the parameters used in this work are shown in Table 1. It is also assumed that these

constants are independent of the temperature in the studied temperature range.

The activity coefficients in the solid phase were calculated using the Wilson equations that consider the combined effects of the differences in molecular size and intermolecular forces.[32] For a binary system, this model is expressed by the following equations

$$\overline{\gamma}_A = \exp(1 - \ln(y_A + (1 - y_A)\Lambda_{AB})) - \left(\frac{y_A}{y_A + (1 - y_A)}\right)\Lambda_{AB} - \left(\frac{(1 - y_A)\Lambda_{BA}}{(1 - y_A) + y_A\Lambda_{BA}}\right) \quad (16)$$

$$\overline{\gamma}_B = \exp(1 - \ln((1 - y_A) + y_A\Lambda_{BA})) - \left(\frac{1 - y_A}{(1 - y_A) + y_A\Lambda_{BA}}\right) - \left(\frac{y_A\Lambda_{AB}}{y_A + (1 - y_A)\Lambda_{AB}}\right) \quad (17)$$

where Λ_{AB} and Λ_{BA} are the Wilson binary interaction parameters defined such that $A \neq B$ for a nonideal exchanger phase, which are a function of temperature. If the activity coefficients of the components are expressed in infinitely dilute mixtures of each component

$$\ln \overline{\gamma}^{\infty}_A = 1 - \ln \Lambda_{AB} - \Lambda_{BA} \quad (18)$$

$$\ln \overline{\gamma}^{\infty}_B = 1 - \ln \Lambda_{BA} - \Lambda_{AB} \quad (19)$$

and additionally the Robinson−Gilliland equation is valid[33]

$$T \ln \overline{\gamma}^{\infty}_i = \text{constant} \quad (20)$$

Then the relationship between the Wilson parameters and the temperature can be expressed as[33]

$$T(1 - \ln \Lambda_{AB} - \Lambda_{BA}) = C^A_{AB} \quad (21)$$

$$T(1 - \ln \Lambda_{BA} - \Lambda_{AB}) = C^B_{AB} \quad (22)$$

where T is the absolute temperature and CAB^A and CAB^B are the constants of the Robinson and Gilliland relationship.

The standard thermodynamic properties of each binary system were obtained using the following thermodynamic relationships[21,34–36]

$$\Delta G^\circ_{AB} = -\frac{RT}{\alpha\beta} \ln K_{AB} \quad (23)$$

$$\Delta G^\circ_{AB} = \Delta H^\circ_{AB} - T \cdot \Delta S^\circ_{AB} \quad (24)$$

where R is the ideal gas constant and ΔG°, ΔH°, and ΔS° are changes in free energy, enthalpy, and entropy, respectively.

From the above two equations,

$$K_{AB}(T) = \frac{1}{e^{\left(\frac{\alpha\beta}{R}\right)\cdot\left[\frac{\Delta H^\circ_{AB}}{T} - \Delta S^\circ_{AB}\right]}} \quad (25)$$

The equilibrium experimental data for the three temperatures studied were fitted together. In this set of equations, the nine unknown parameters (maximum capacity (q_0), Wilson param-

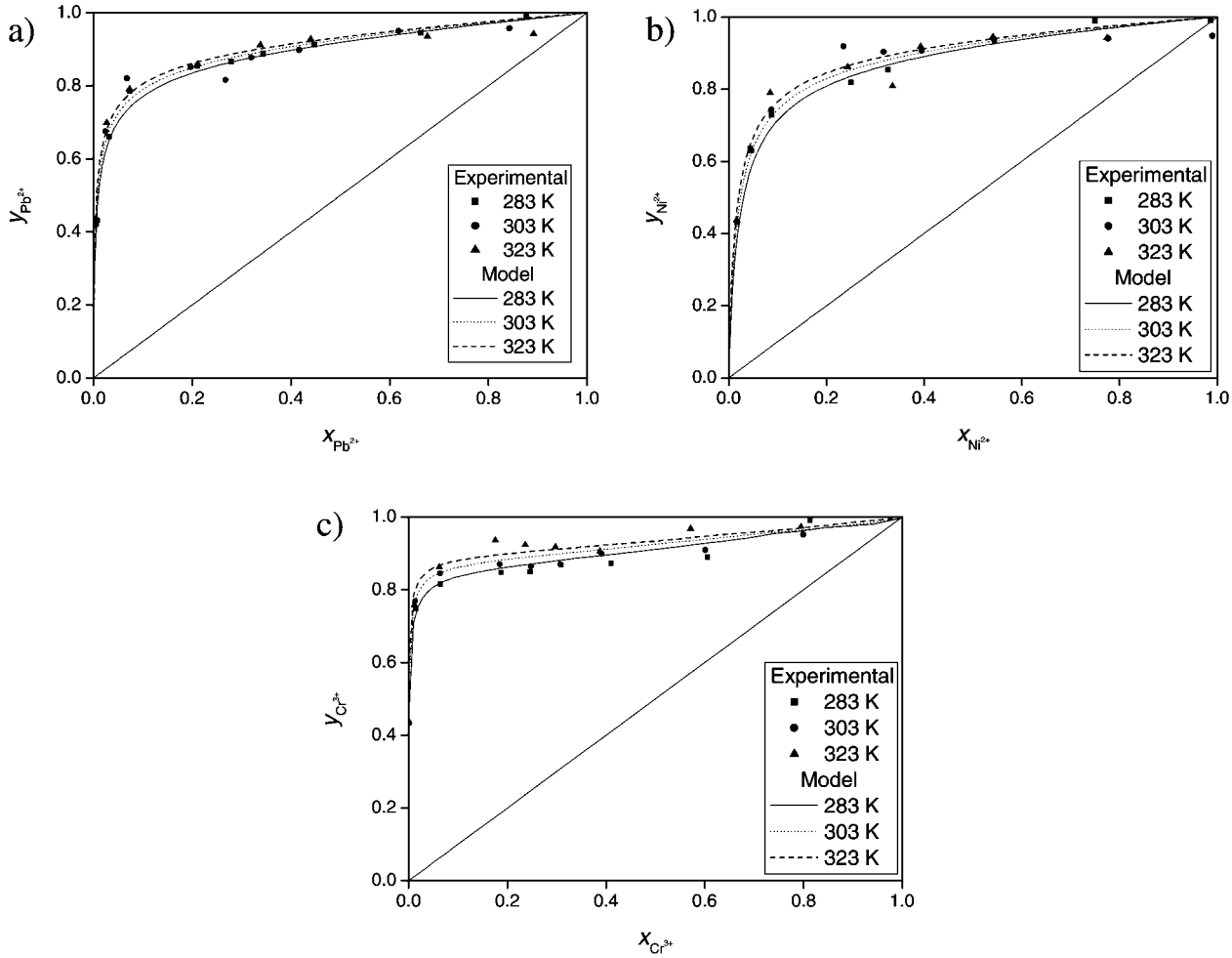

Figure 1. Equilibrium isotherms of H^+/Pb^{2+}, H^+/Ni^{2+}, and H^+/Cr^{3+} with Amberlite IR-120 at $N = 0.1$ eq·L^{-1}. (a) System H^+/Pb^{2+}. (b) System H^+/Ni^{2+}. (c) System H^+/Cr^{3+}.

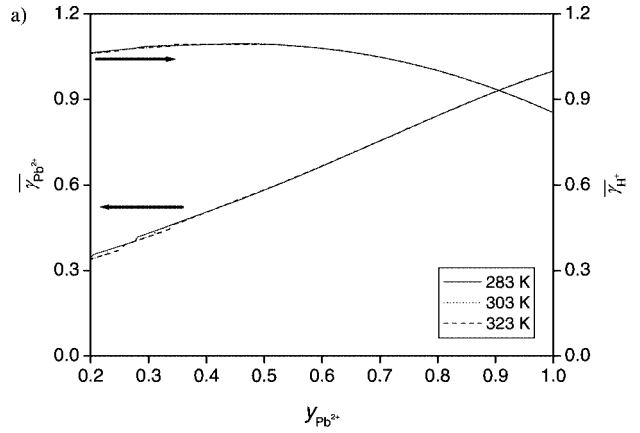

Figure 2. Activity coefficients in the resin phase. (a) System H^+/Pb^{2+} for a temperature of (283, 303, and 323) K. (b) Systems H^+/Pb^{2+}, H^+/Ni^{2+}, and H^+/Cr^{3+} for a temperature of 303 K.

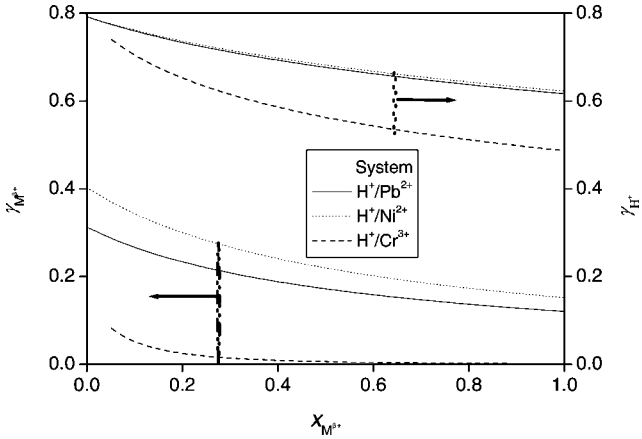

Figure 3. Activity coefficients in the liquid phase for the systems H^+/Pb^{2+}, H^+/Ni^{2+}, and H^+/Cr^{3+} at 303 K.

eters (Λ_{AB} and Λ_{BA}) at each temperature, and both the thermodynamic properties ($\Delta H°$ and ΔS °)) were obtained by fitting the experimental data to the model. To solve the model, it was also taken into account that the Wilson parameter is subjected to the Robinson−Gilliland constraint. A nonlinear regression method based on the Marquardt algorithm, described in previous works,[34,37] has been used to obtain the mentioned parameters.

Results and Discussion

Two different values for the resin capacity were obtained: 5.56 meq·g^{-1} for the ions lead and nickel and 5.3 meq·g^{-1} for chromium. These values are a little higher than the value obtained of 5.0 meq·g^{-1} for the ions Cu^{2+}, Cd^{2+}, and Zn^{2+} by Valverde et al.[17] The difference in the capacity obtained for chromium and for lead and nickel could be attributed to dissociation effects or exclusion phenomena. In this context, the pH value of a solution is an important factor that can control the uptake of the species in solution.[38]

Table 6. Standard Thermodynamic Properties of the Binary Systems H^+/Pb^{2+}, H^+/Ni^{2+}, and H^+/Cr^{3+} on the Resin Amberlite IR-120

system	T / K	$\Delta G°_{AB}$ / kJ·mol^{-1}	$\Delta H°_{AB}$ / kJ·mol^{-1}	$\Delta S°_{AB}$ / J·mol^{-1}·K^{-1}
H^+/Pb^{2+}	283	−1.5052	4.6624	21.7822
	303	−1.9408		
	323	−2.3765		
H^+/Ni^{2+}	283	0.3465	4.6625	15.2428
	303	0.0416		
	323	−0.2632		
H^+/Cr^{3+}	283	−1.1396	7.6861	31.1697
	303	−1.7630		
	323	−2.3864		

The equilibrium experiments for nickel and lead were always carried out at pH < 2, conditions at which both ions are entirely found as Ni(II) and Pb(II), respectively. The experiments with chromium were carried out at pH values lower than three. According to Kocaoba and Akcin,[39] in this pH region, two species of chromium can be found, mainly Cr(III) (91.9 %) and also the complex $Cr(OH)^{2+}$ (7.7 %). Thus, the resin could uptake selectively both forms of chromium. Nevertheless, the lower valence of the $Cr(OH)^{2+}$ would allow the exchanger to uptake a higher amount of moles of this species than the Cr(III). In the theoretical treatment, the total amount of chromium exchanged was considered as Cr(III), and the useful capacity obtained was slightly lower than 5.6 meq·g^{-1} indicating that the resin prefers this form of chromium from the liquid solution. The difference between the maximum usable capacities exhibited by the resin for the studied ions could be related with the hydrated ionic radius.

The hydrated ionic radius of the three metals in this study decrease in the order Cr(III) > Pb(II) > Ni(II).[40,41] Chromium(III) has the largest hydrated ionic radius of any known heavy metal, and its exchange requires a favorable pore opening.[35] It is possible that the total active centers of the exchanger are not available for this species, thus diminishing the useful resin capacity. On the other hand, the result obtained by Demirbas et al.[34] for Pb^{2+} and Ni^{2+} indicates that the pH has a strong influence on the removal of both ions since this resin exhibits different capacities for both ions at higher pH values. These results indicate that the behavior of this resin for these kinds of ions is dependent strongly on pH since hydroxyl complexes form mainly at higher pH values and the hydrated size of the ionic species.

The experimental data and the theoretical data from the model are shown in Tables 2 to 4. Likewise, Table 5 contains the equilibrium constant (K_{AB}) and the binary interaction parameters of Wilson (Λ_{AB} and Λ_{BA}) and the constants of the Robinson and Gilliland relationship. The average deviation from the experimental data was calculated from the difference, in absolute value (Abs), between the experimental concentration of the metal ion in the resin and that predicted by the model, according to the following formula

$$\text{av. dev. } (\%) = \frac{\sum_{i=1}^{m} Abs\left(\frac{y_{M^{+\beta}}^{\text{exptl}} - y_{M^{+\beta}}^{\text{theor}}}{y_{M^{+\beta}}^{\text{exptl}}}\right) \times 100}{m} \qquad (26)$$

where m is the number of experimental data of each isotherm.

The average deviation is lower than 4.5 % in most cases. The values obtained from modeling calculations were used to plot the theoretical equilibrium isotherms. The model predictions for each of the systems at each temperature are compared graphically with the experimentally determined equilibrium points in Figure 1. As can be seen, the theoretical results are in quite good agreement with the experimental data. Although the ion-exchange equilibrium curves for different metal ions varied minutely among the temperatures, a common trend toward a move away from the diagonal as the temperature increases was observed. This indicates that temperature favors counterion uptake from the liquid phase. According to the values of the equilibrium constants obtained, the Amberlite IR-120 exhibits the following order of selectivity, $Cr^{3+} > Pb^{2+} > Ni^{2+}$, in all ranges of temperature studied. Besides, all the isotherms are in the upper diagonal confirming the general rule of a bigger affinity of artificial resins for ions of higher valence.[17,23]

The activity coefficients in the solid phase for the system H^+/Pb^{2+} at different temperatures are shown in Figure 2a. As can be seen, the effect of the temperature on the activity coefficient for both cations in this phase is practically negligible. On the other hand, Figure 2b indicates that the activity coefficients in the solid phase depend strongly on the characteristics of the ions involved in the ion-exchange process.

Figure 3 shows the behavior of the activity coefficient in the liquid phase for the systems under study at 303 K. As can be seen, the values are far from one indicating that the behavior of these ions is nonideal in this phase: mainly the ion chromium. Taking into account the trend of activity coefficients for all ions in both phases, it is possible to conclude that the studied systems are nonideal and require a real treatment for both phases.

Table 6 contains the thermodynamic properties of the binary systems constituted by H^+/Pb^{2+}, H^+/Ni^{2+}, and H^+/Cr^{3+} at (283, 303, and 323) K. The positive enthalpy indicates that these processes are endothermic which differs with the normal behavior of an ion-exchange process. In the same way, the standard entropy obtained is also positive, indicating an increase in the degree of freedom of the loaded species. Nevertheless, the negative standard free energy clearly indicates that the process is spontaneous, and the metal cations are preferably bound to the resin as compared to protons. This preference increases with temperature as was discussed above.

Conclusions

Ion-exchange equilibrium H^+/Pb^{2+}, H^+/Ni^{2+}, and H^+/Cr^{3+} systems using strongly acidic cationic resin Amberlite IR-120 have been measured at (283, 303, and 333) K. Experimental equilibrium data can be satisfactorily correlated to the homogeneous mass action model (LAM) using the Wilson and Pitzer limiting law equations to calculate activity coefficients in the solid phase and in the liquid phase, respectively. Theoretical results are in good agreement with experimental ones. The temperature of the reaction has a slight influence on the equilibrium behavior. The resin presents a higher capacity of uptake for lead and nickel than chromium, but this behavior can be related with the largest hydrated ionic size of Cr(III) that can promote its ion exclusion as well as the contact with the total resin active centers. The standard free energy was negative, indicating the spontaneity of the process and that the resin prefers the metal ions to protons. Finally, the resin exhibits the following selectivity order: Cr(III) > Pb(II) > Ni(II) ≫ H^+.

Literature Cited

(1) Kandah, M. S.; Meunier, J-L. Removal of nickel ions from water by multi-walled carbon nanotubes. *J. Hazard. Mater.* **2007**, *146*, 283–288.

(2) Lao, C.; Zeledón, Z.; Gamisans, X.; Solé, M. Sorption of Cd(II) and Pb(II) from aqueous solutions by a low-rank coal (Leonardite). *Sep. Purif. Technol.* **2005**, *45*, 79–85.

(3) Jouad, El M.; Jourjon, F.; Le Guillanton, G.; Elothmani, D. Removal of metal ions in aqueous solutions by organic polymers: use of a polydiphenylamine resin. *Desalination* **2005**, *180*, 271–276.

(4) Kurniawan, T. A.; Chan, G.; Lo, W-H.; Babel, S. Physico-chemical treatment techniques for wastewater laden with heavy metals. *Chem. Eng. J.* **2006**, *118*, 83–98.

(5) Öztürk, A. Removal of nickel from aqueous solution by the bacterium Bacillus thuringiensis. *J. Hazard. Mater.* **2007**, *147*, 518–523.

(6) Romera, E.; González, F.; Ballester, A.; Blázquez, M. L.; Muños, J. A. Comparative study of biosorption of heavy metals using different types of algae. *Bioresource* **2007**, *98*, 3344–3353.

(7) Rao, K. S.; Sarangi, D.; Dash, P. K.; Chandhury, G. R. Treatment of wastewater containing copper, zinc, nickel and cobalt using Duolite ES-467. *J. Chem. Technol. Biotechnol.* **2002**, *77*, 1107–1113.

(8) Dąbrowski, A.; Hubicki, Z.; Podkościelny, P.; Robens, E. Selective removal of the heavy metal ions from waters and industrial wastewaters by ion-exchange method. *Chemosphere* **2004**, *56*, 91–106.

(9) Patterson, J. W. *Metal Speciation Separation and Recovery*; Lewis Publishers: Chelsea, 1987.

(10) Frederick, K. Countercurrent regeneration: principles and applications. *Ultrapure Water* **1996**, 53–56.

(11) Bailey, S. E.; Olin, J. T.; Bricka, R. M.; Adrian, D. D. A review of potentially low-cost sorbents for heavy metals. *Water Res.* **1999**, *33*, 2469–2479.

(12) Valverde, J. L.; de Lucas, A.; Carmona, M.; Pérez, J. P.; González, M.; Rodríguez, J. F. Minimizing the environmental impact of the regeneration process of an ion exchange bed charged with trasition metals. *Sep. Purif. Technol.* **2006**, *49*, 167–173.

(13) Kokaoba, S.; Akcin, G. Removal chromium (III) and cadmium (II) from aqueous solutions. *Desalination* **2005**, *49*, 151–156.

(14) Valverde, J. L.; de Lucas, A.; Carmona, M.; González, M.; Rodríguez, J. F. Model for the determinination of diffusion coefficients of heterovalent ions in macroporous ion exchange resins by zero-length column method. *Chem. Eng. Sci.* **2005**, *60*, 5836–5844.

(15) Cavaco, S. A.; Fernandes, S.; Quina, M. M.; Ferreira, L. M. Removal chromium from electroplating industry effluents by ion exchange resins. *J. Hazard. Mater.* **2007**, *144*, 634–638.

(16) Skogley, E. O.; Dobermann, A. Synthetic ion-exchange resins: soil and environmental studies. *J. Environ. Qual.* **1996**, *25*, 13–24.

(17) Valverde, J. L.; de Lucas, A.; González, M.; Rodríguez, J. F. Equilibrium data for the exchange of Cu^{2+}, Cd^{2+}, and Zn^{2+} ions on the cationic exchanger Amberlite IR-120. *J. Chem. Eng. Data* **2001**, *47*, 613–617.

(18) Valverde, J. L.; de Lucas, A.; Carmona, M.; González, M.; Rodríguez, J. F. A generalized model for the measurement of effective diffusion coefficients ions in ion exchangers by zero-length column method. *Chem. Eng. Sci.* **2004**, *59*, 71–79.

(19) Shallcross, D. C.; Herrmann, C. C.; McCoy, B. J. An improved model for the prediction of multicomponent ion exchange equilibria. *Chem. Eng. Sci.* **1988**, *43*, 279–288.

(20) Mehablia, M. A.; Shallcross, D. C.; Stevens, G. W. Prediction of multicomponent ion exchange equilibria. *Chem. Eng. Sci.* **1994**, *49*, 2277–2286.

(21) Ioannidis, S.; Anderko, A.; Sanders, S. J. Internally consistent representation of binary ion exchange equilibria. *Chem. Eng. Sci.* **2000**, *55*, 2687.

(22) Mumford, K. A.; Northcott, K. A.; Shallcross, D. C.; Stevens, G. W.; Snape, I. Development of a two parameter temperature-dependent semi-empirical thermodynamic ion exchange model using binary equilibria with Amberlite IRC 748 resin. *Ind. Eng. Chem. Res.* **2007**, *46*, 3766–3773.

(23) de Lucas, A.; Zarca, J.; Cañizares, P. Ion-exchange equilibrium of Ca^{2+}, Mg^{2+}, K^+, Na^+ and H^+ ions on Amberlite IR-120: Experimental determination and theoretical prediction of the ternary and quaternary equilibrium data. *Sep. Sci. Technol.* **1992**, *27*, 823–841.

(24) de Lucas, A.; Cañizares, P.; García, M. A.; Gómez, J.; Rodríguez, J. F. Recovery of nicotine from aqueous extracts of tobacco wastes by an H^+-form strong-acidion exchanger. *Ind. Eng. Chem. Res.* **1998**, *37*, 4783–4791.

(25) Velayudhan, A.; Horvath, C. Adsorption and ion exchange isotherms in preparative chromathography. *J. Chromatogr. A* **1994**, *663*, 1–10.

(26) Vo, B. S.; Shallcross, D. C. Modeling solution phase behaviour in multicomponent ion exchange equilibrium involving H^+, Na^+, K^+, Mg^{2+}, and Ca^{2+} ions. *J. Chem. Eng. Data* **2005**, *50*, 1995–2002.

(27) Pitzer, K. S. *Activity Coefficients in Electrolyte Solutions*; CRC Press: Boca Raton, 1991.

(28) Pitzer, K. S.; Thermodynamics of electrolytes, I. Theoretical basis and general equations. *J. Phys. Chem.* **1973**, *77*, 268–277.

(29) Lin, L. Ch.; Juang, R. Sh. Ion-exchange equilibria of Cu(II) and Zn(II) from aqueous solutions with Chelex 100 and Amberlite IRC 748 resins. *Chem. Eng. J.* **2005**, *112*, 211–218.

(30) Pitzer, K. S.; Mayorga, G. Thermodynamics of electrolytes II. Activity and osmotic coefficients for strong electrolytes with one or both ions univalent. *J. Phys. Chem.* **1973**, *77*, 2300–2308.

(31) Sadowska, T.; Libus, W. Thermodynamics properties and solution equilibria of aqueous bivalent transition metal nitrates and magnesium nitrate. *J. Solution Chem.* **1982**, *11*, 457–468.

(32) Wilson, G. M. Vapor-liquid equilibria XI. A new expression for the excess free energy of mixing. *J. Am. Chem. Soc.* **1964**, *86*, 127–130.

(33) Robinson, C.; Gilliland, E. *Elements of fractional destilation*; McGraw-Hill: New York, 1950.

(34) de Lucas, A.; Zarca, J.; Cañizares, P. Ion-exchange equilibrium in a binary mixture. Models for its characterization. *Inter. Chem. Eng.* **1994**, *34*, 486–497.

(35) El-Shahat, M. F.; Saad, E. A.; Burham, N.; El-Naggar, I. M. Ion-exchange equilibria between some rare earth metal ions and hydrogen ions in iron(III) and tin(IV) antimonates as cation exchangers. *Microchem. J.* **1998**, *60*, 95–100.

(36) Ivanov, M. V.; Timofeevskaja, V. D.; Gavlina, O. T.; Gorshkov, V. I. Dual-temperature reagent-less ion-exchange separations of alkali metal salts on zeolites. *Microporous Mesoporous Mater.* **2003**, *65*, 257–265.

(37) de Lucas, A.; Valverde, J. L.; Cañizares, P.; Rodriguez, L. Ion Exchange Equilibria of DL-Lisine Monohydrochloride on Amberlite IRA 420. *Solvent Extr. Ion Exch.* **1995**, *13*, 1123–1143.

(38) Gode, F.; Pehlivan, E. A comparative study of two chelating ion-exchange resin for the removal of chromium (III) from aqueous solution. *J. Hazard. Mater.* **2003**, *B100*, 231–243.

(39) Kocaoba, S.; Akcin, G. Removal and recovery of chromium and chromium speciation with MINTEQA2. *Talanta* **2002**, *57*, 23–30.

(40) Demirbas, A.; Pehlivan, E.; Gode, F.; Atun, T.; Arslan, G. Adsorption of Cu(II), Zn(II), Ni(II), Pb(II), and Cd(II) from aqueous solution on Amberlite IR-120 synthetic resin. *J. Colloid Interface Sci.* **2005**, *282*, 20–25.

(41) Covarrubiasa, C.; Arriagada, R.; Yáneza, J.; Garbaland, M. T. Cr(III) exchange on zeolites obtained from kaolin and natural mordenite. *Microporous Mesoporous Mater.* **2006**, *88*, 220–231.

Received for review January 22, 2008. Accepted March 29, 2008.

JE8000552